

PCCP

Accepted Manuscript



This is an *Accepted Manuscript*, which has been through the Royal Society of Chemistry peer review process and has been accepted for publication.

Accepted Manuscripts are published online shortly after acceptance, before technical editing, formatting and proof reading. Using this free service, authors can make their results available to the community, in citable form, before we publish the edited article. We will replace this *Accepted Manuscript* with the edited and formatted *Advance Article* as soon as it is available.

You can find more information about *Accepted Manuscripts* in the [Information for Authors](#).

Please note that technical editing may introduce minor changes to the text and/or graphics, which may alter content. The journal's standard [Terms & Conditions](#) and the [Ethical guidelines](#) still apply. In no event shall the Royal Society of Chemistry be held responsible for any errors or omissions in this *Accepted Manuscript* or any consequences arising from the use of any information it contains.

**Surface texture and physicochemical characterization of
mesoporous carbon – wrapped Pd-Fe catalysts for
low-temperature CO catalytic oxidation**

Weiliang Han, Guodong Zhang, Kun Zhao, Gongxuan Lu*, Zhicheng Tang*

*(National Engineering Research Center for Fine Petrochemical Intermediates, Lanzhou Institute
of Chemical Physics, Chinese Academy of Sciences, Lanzhou, 730000, China)*

*Corresponding author. Tel.: +86-931-4968083, Fax: +86-931-8277088, E-mail
address: tangzhicheng@licp.cas.cn (Z.Tang).

Abstract

In this paper, mesoporous carbon (meso-C) with three-dimensional mesoporous channels had been synthesized through a nanocasting route using three-dimensional mesoporous silica KIT-6 as the template. Mesoporous carbon wrapped Pd-Fe nanocomposite catalysts were synthesized by co-precipitation method. The effects of experimental conditions, such as pH value, Fe loading content and calcined temperature, on CO oxidation were studied in detail. The prepared Pd-Fe/meso-C catalysts showed excellent catalytic activity by optimized the experimental conditions. The surface tetravalent Pd content, existing form of Fe species, surface chemical adsorbed oxygen concentration, and the pore channel of mesoporous carbon played vital roles in achieving the highest performance over the Pd-Fe/meso-C catalyst. The reaction pathway was conjectured according to the XPS analysis of Pd-Fe/meso-C catalysts on CO oxidation, which maybe adhered to the Langmuir-Hinshelwood +

Redox mechanism. The effect of moisture on CO conversion was investigated, and the superior Pd-Fe/meso-C catalyst could maintain its activity beyond 12h. This catalyst also showed excellent activity than the reported value in the existed literature.

Key words: Nanocasting route; Pd-Fe catalyst; Mesoporous carbon; CO oxidation; Key factor

1. Introduction

CO is one of the major air pollutants and it is a colorless, odorless gas which can be emitted from a large number of sources. Its presence even in traces can cause the serious environmental and health problems. Thus, control of CO in the air has been an important area of research. From the viewpoint of environmentalists, catalytic CO oxidation has been regarded as an effective way to remove CO [1-4]. In the next place, CO oxidation reaction constitutes a prime example of a nonequilibrium system that exhibits a rich variety of behavioral patterns and complex irreversible critical behaviors [5-6]. Hence, catalysis oxidation for CO has attracted much attention in the past decade.

Pd-Fe based catalysts have high performance for low temperature CO catalytic oxidation [7-13]. Such as, Lu et al. [8] prepared Pd-Fe-Ox catalysts supported on SBA-15, CeO₂ nano-particles with rich (111) facets and CeO₂ nano-rod with rich (200) facets. The results showed that when CeO₂ nano-rod was used as a support, Pd-Fe-Ox catalyst exhibits higher activity ($T_{100}=10$ °C), resulting from the rich (200) facets of CeO₂ nano-rod, which leads to a formation of large numbers of the oxygen vacancies

on the surface of Pd-Fe-Ox catalysts. Satauma et al. [10] also investigated the effect of supports (CeO_2 , TiO_2 , Al_2O_3 , ZrO_2 , and SiO_2) on CO oxidation over Pd catalysts at low temperature, and the results indicated that higher reducibility of supported Pd to metallic species was one of the activity-controlling factors for the oxidation activity. In our previous research, a series of Pd-Fe/carbon sphere (CS) catalysts were prepared by a co-precipitation method and applied in low-temperature CO oxidation reactions, it was discovered that the particle sizes of carbon spheres, calcination temperatures of catalysts, Pd loadings and H_2 reduction, etc, have important effect on catalytic activities for CO oxidation [13]. In these literatures, the support had important influence on the catalytic performance for low temperature CO catalytic oxidation.

Due to remarkable chemical and physical properties such as uniform and tunable pore sizes, high surface area and open-framework structures, mesoporous carbon have been recognized to play an increasingly important role in heterogeneous catalysis processes as catalyst support [14-20]. Dong et al. [14] prepared Novel ordered mesoporous carbon nitride (MCN)-supported Pt catalysts, the result indicated that the basicity of the supports is helpful for promoting the oxidation of glycerol to glyceraldehyde and further oxidation to glyceric acid. We synthesized three kinds of carbon materials as supports, i.e., carbon sphere (non-C), microporous carbon (micro-C) and mesoporous carbon (meso-C), the Pd/meso-C catalysts with impregnation method exhibited the highest catalytic activity because meso-C supports had the well-ordered mesoporous structure, large BET surface area, porous channels and higher dispersion of Pd nanoparticle [17].

In this paper, mesoporous carbon (meso-C) was synthesized and supported Pd-Fe was applied to CO oxidation. The effect of pH value, Pd loading content and calcination temperature on low temperature CO catalytic oxidation was studied in detail. Their properties were characterized by XRD, BET, TEM and XPS techniques.

2 Experimental

2.1 Synthesis of KIT-6

Mesoporous KIT-6 was synthesized according to the previously reported method [21]. Typically, 6.0g P123 (EO₂₀PO₇₀EO₂₀, MW=5800, Aldrich) was dissolved in 217g distilled water and 11.8g 35 wt.% HCl solution with stirring at 35 °C. After the dissolution completed, 6.0g n-BuOH was added at once. Stirring for an hour, 12.9g TEOS was added to the homogeneous clear solution and the obtained mixture was left under vigorous and constant stirring at 35 °C for 24h. Then, the solution was transferred to a Teflon-lined stainless steel autoclave at 100 °C for 24h. Finally, the product was dried at 100 °C and calcined at 550 °C for 5h to completely eliminate the template. The white mesoporous KIT-6 powder was obtained.

2.2 Synthesis of carbon material

In a typical synthesis of mesoporous carbon (meso-C), 2.97g of glucose was dissolved in 15ml distilled water with stirring at room temperature. After complete dissolution, 1g mesoporous silica template (KIT-6) was added. The mixture was stirred at 80 °C until a nearly dry powder had been obtained. The sample was then heated slowly to 750 °C with a ramp 2 °C min⁻¹ and calcined at the same temperature for 5 h to carbonize the glucose. The resulting sample was twice treated with a hot

2 molL⁻¹ NaOH solution to remove the silica template, followed by washing with water and ethanol several times, and then drying at 60 °C.

2.3 Catalyst preparation

Pd-Fe/meso-C catalysts were prepared by co-precipitation method. 0.5 g meso-C were firstly suspended in the mixture aqueous solution of Pd(NO₃)₂ and Fe(NO₃)₃. Then 0.4 mol/L Na₂CO₃ solutions were gradually added into the above suspended solution to adjust the pH value of the mixed solution. After stirring for 3 h, the mixture was filtered and washed with distilled water. The resulting solid was dried and calcined. The pH value was changed from 7.5 to 9.5. The Pd loading content was 0.33 wt.%~1.00 wt.% in this paper. The calcined temperature of catalyst was 100 °C~400 °C.

2.4 Catalyst Characterization

Powder X-ray diffraction (XRD) analysis was performed to verify the crystallographic phases present in supports and catalysts. XRD patterns of the samples were recorded on a Rigaku D/MAX-RB X-ray diffractometer with a target of Cu K α operated at 60 kV and 55 mA with a scanning speed of 0.5 °/min. The 2 θ of wide-angle ranged from 20-80°.

Chemical states of the atoms in the catalyst surface were investigated by X-ray photoelectron spectroscopy (XPS) on a VG ESCALAB 210 Electron Spectrometer (Mg K α radiation; $h\nu = 1253.6$ eV). XPS data were calibrated using the binding energy of C1s (284.6 eV) as the standard.

Transmission electron microscopy (TEM) experiments were carried out to study

the fine morphology of the carbon material, using a FEI TECNAIG² Microscope operated at 200 kV.

The specific surface area and the average pore diameter of the catalysts were determined by nitrogen adsorption in accordance with the BET method, with a Micromeritics ASAP 2010 instrument. Prior to measurements, the samples were degassed at 150 °C for 6 h.

2.5 Measurements of catalytic performance

Catalytic activity tests were performed in a continuous-flow fixed-bed microreactor. A glass tube with an inner diameter of 6 mm was chosen as the reactor tube. About 300 mg catalyst with the average diameter of 20~40 mesh was placed into the tube. The reaction gas mixture consisting of 1 vol.% CO balanced with air was passed through the catalyst bed at a total flow rate of 50 mlmin⁻¹. A typical weigh hourly space velocity (WHSV) was 10000 mlg⁻¹h⁻¹. The composition of the influent and effluent gas was detected with an online GC-7890II gas chromatograph equipped with a thermal conductivity detector and a molecular sieve 5A column. As we all know, CO oxidation reaction is accompanied by a reduction in the number of moles. In this paper, this change of moles was neglected. Therefore, the CO conversion rate (X_{CO}) was calculated:

$$X_{CO} = \frac{([\text{CO}]_{\text{in}} \text{vol.}\% - [\text{CO}]_{\text{out}} \text{vol.}\%)}{[\text{CO}]_{\text{in}} \text{vol.}\%} \times 100$$

The $[\text{CO}]_{\text{in}}$ and $[\text{CO}]_{\text{out}}$ was CO concentration (vol.%) in gas mixture before and after CO oxidation reaction, respectively.

The hydrothermal pretreatment process was carried out as follows. The reaction

gas mixture was passed through water reactor, and then flowed through the catalyst bed at a total flow rate of 50 mlmin⁻¹. The composition of the influent and effluent gas was detected with an online GC-7890II gas chromatograph.

3 Result and discussion

In this paper, mesoporous carbon (meso-C) was synthesis by the hard template method. It was used as support and a series of Pd-Fe/meso-C catalysts were successfully prepared by co-precipitation method and applied to low temperature CO oxidation. The effect of loading Pd-Fe on surface area and pore structure was investigated in detail.

3.1 Preparation of meso-C support and Pd-Fe/meso-C catalyst

Table 1 summarizes BET surface areas, microporous area, external surface area, pore volumes and average pore diameters of meso-C support and Pd-Fe/meso-C catalyst. From Table 1, the meso-C sample had superior surface area, the value was 699.50 m²g⁻¹, and the external surface area of meso-C sample was far higher than microporous area, which meant that the meso-C support was a large number mesoporous and a little microporous. After loading Pd-Fe, the surface area and external surface area of sample had fallen, the microporous area was even disappeared. This indicated that Pd-Fe was loaded on meso-C support surface and pore channel.

Fig.1A and Fig.1B show the N₂ adsorption-desorption isotherms and BJH pore size distributions of meso-C support and Pd-Fe/meso-C catalyst, respectively. According to the Brunauer, Deming, Deming and Teller (BDDT) classification, the N₂ adsorption-desorption isotherm of meso-C support was belonged to the typical

type-IV curve with N_2 hysteresis loop, accompanied with the sharp capillary condensation at the relative pressure P/P_0 of 0.42-0.80. After loaded Pd-Fe, the N_2 adsorption-desorption isotherm of Pd-Fe/meso-C catalyst also displayed the type-IV curves with the obvious capillary condensation at the 0.42-0.90. From Fig.2B, the pore sizes of meso-C support were mainly distributed in two ranges of 1.7-2.0nm and 2.0-9.0 nm, which indicated that the meso-C sample had both mesoporous and microporous structure. This result was same as the result of Table 1. But the peak of the pore size from 1.7 to 2.0 nm was disappeared after loaded Pd-Fe, which showed that Pd-Fe was loaded on meso-C support pore channel.

Fig.2 shows the TEM image of meso-C support and Pd-Fe/meso-C catalyst. From Fig.2A, meso-C sample exhibited a well-ordered pore structure, indicating that meso-C highly duplicates the ordered structure of KIT-6 in the preparation process. After loaded Pd-Fe, the well-ordered pore structure reduced, which indicated that Pd-Fe had been loaded on meso-C support surface and pore channel. This was main reason that the surface area, external surface area of sample had fallen and the microporous area was even disappeared.

3.2 The effect of pH value on the activity of CO oxidation

The effect of reaction pH values on catalytic activity of Pd-Fe/meso-C catalyst was investigated and the results were shown in Fig.3 (the Pd loading content was 0.625 wt.%, the calcined temperature was 200 °C). From Fig.3, The total conversion temperature (T_{100}) decreased with the increase of reduction pH values at first, and then decreased. At pH 8.5, the catalytic activity was the best, T_{100} was 30 °C. In order

to investigate the effect of reduction pH values on catalytic activity, the catalysts were characterized by XPS.

As we all know, CO catalytic oxidation is a surface reaction, so chemical states of surface atoms in catalysts as well as composition and related distribution of the surface elements, active phases of the catalysts which involved CO oxidation and variation of the surface species during catalytic reaction, etc, is important part to analysis catalyst activity. XPS was used to demonstrate above mention surface properties of catalysts, and the result was seen in Fig.4. Fig.4A showed the Pd element on the surface of Pd-Fe/meso-C-7.5, Pd-Fe/meso-C-8.5 and Pd-Fe/meso-C-9.5 catalysts, respectively. Two peaks of Pd $3d_{5/2}$ appeared at binding energies of 337.7-337.9eV and 336.0-336.4eV in all catalysts. It was indicated that there were two kinds of palladium species (bivalent Pd and tetravalent Pd) and they were coexisted on the surface of Pd-Fe/meso-C-7.5, Pd-Fe/meso-C-8.5 and Pd-Fe/meso-C-9.5 catalysts [22, 23]. According to our previous research [13, 17], tetravalent Pd was main active component in Pd-Fe based catalysts on CO oxidation. The calculated percentages of tetravalent Pd are listed in Table 2. From Table 2, the surface Pd⁴⁺ content order was following: Pd-Fe/meso-C-8.5 (0.165 wt.%)> Pd-Fe/meso-C-9.5 (0.103 wt.%)> Pd-Fe/meso-C-7.5 (0.074 wt.%). Contrast with Fig.4A and Fig.3, it was discovered that the activity of catalyst increased with the surface tetravalent Pd content increased. This was also indicated that tetravalent Pd was main active component in Pd-Fe/meso-C catalysts on CO oxidation.

Fig.4B shows the O element on the surface of Pd-Fe/meso-C-7.5,

Pd-Fe/meso-C-8.5 and Pd-Fe/meso-C-9.5 catalysts, respectively. Three peaks at 529.9-530.5 eV (O), 532.0-532.2 eV (O') and 533.5-533.8 eV (O'') could be identified by the deconvolution of the O1s spectra. They were assigned to O²⁻ in the catalysts lattice, surface adsorbed oxygen such as O⁻ or OH⁻ and adsorbed molecular water [24, 25], respectively. The surface oxygen concentration and surface adsorbed oxygen concentration play a significant role on CO catalytic oxidation reaction. The relative content of the surface adsorbed oxygen species in the total surface oxygen can be estimated from the relative area of the sub-peak, the results are shown in Table 2. It was clearly seen in Table 2 that the Pd-Fe/meso-C-8.5 catalyst possessed the highest surface oxygen concentration and surface adsorbed oxygen concentration than Pd-Fe/meso-C-7.5 and Pd-Fe/meso-C-9.5 catalysts. This was also an important reason that the Pd-Fe/meso-C-8.5 catalyst had superior activity on CO oxidation.

3.3 The effect of Pd content on the activity of CO oxidation

As we all know, Pd species were the main active component in Pd-Fe based catalysts on CO oxidation. So the influence of Pd loading content on reaction results of CO oxidation were studied, the results are seen in Fig.5 (the reaction pH value was 8.5, the calcined temperature was 200 °C). Obviously, Pd-Fe/meso-C catalysts exhibited high activity for CO oxidation. The reaction activity increased gradually with the increase of Pd loading content. However, the enhancement of Pd-Fe/meso-C catalysts activity is not linearly proportional to the Pd loading, particularly over the catalyst containing a relatively high amount of Pd above 0.625 wt.%.

3.4 The effect of calcined temperature on the activity of CO oxidation

The effect of calcination temperature on the performance of Pd-Fe/meso-C sample was studied by varying the calcination temperature in a range from 100 to 400 °C, the results of which are shown in Fig.6. The catalyst was marked as Pd-Fe/meso-C-x (the Pd loading content was 0.625 wt.%, the reaction pH value was 8.5, x=calcined temperature). It was seen in Fig.6 that T_{100} was increased at first, and then decreased along with rose of calcined temperature of catalysts. The catalyst calcined at 200 °C had superior activity on CO oxidation, T_{100} was 25 °C. The reason of above result is studied by XRD and XPS characterization.

Fig.7 shows the XRD patterns of Pd-Fe/meso-C catalysts with varying the calcination temperature in a range from 100 to 400 °C. From Fig.7, no characteristic diffraction peaks of Pd particles appeared in all catalysts, which indicated that the Pd-Fe/meso-C sample calcined at 100-400 °C possessed highly dispersed of Pd nanoparticles. Only one broad peak at 35.7° appeared in Fig.7a, which was assigned to (211) crystalline plane of FeO(OH) (JCPDS PDF#18-0639) according the literature [13]. With the increase of calcination temperature, the peak at 35.7° strengthened (seen Fig.7b). Further increase of calcination temperature, two Fe₂O₃ species were observed from Fig.7c. The peaks at 35.6°, 43.2° and 53.7° was assigned to maghemite-C (JCPDS PDF#39-1346), and other peaks at 24.1°, 33.1°, 35.6°, 49.4°, 54.1°, 57.6°, 62.4° and 64.0° was assigned to hematite (JCPDS PDF#33-0664). From Fig.7d, the characteristic peak at Fig.7c enhanced and the peak at 40.8° appeared, which was assigned to (113) crystalline plane of hematite (JCPDS PDF#33-0664). Calcination process of catalysts was the process of transformation from FeO(OH) to

iron oxide. By comparing the result of Fig.6, it was observed that FeO(OH) species were helpful for the increase of activity.

Fig.8 shows the XPS spectra of Pd-Fe/meso-C catalysts with varying the calcination temperature in a range from 100 to 400 °C. The Pd element on the surface of Pd-Fe/meso-C sample calcined at 100-400 °C was shown in Fig.8A. From Fig.8Aa, it was existed two palladium species (bivalent Pd and tetravalent Pd). With increase of calcination temperature, the bivalent Pd species was disappeared. The calculated percentages of tetravalent Pd are listed in Table 3. The tetravalent Pd content was 0.165, 0.246, 0.250, 0.273 wt.% When calcined temperature was 100, 200, 300 and 400 °C, respectively. The surface tetravalent Pd content increased with the increased of calcined temperature.

Fig.8B shows O element on the surface of Pd-Fe/meso-C sample calcined at 100-400 °C. It was clearly noticed that three peaks (O, O', O'') also could be identified by the deconvolution of the O1s spectra. The binding energy at 529.9-530.5 eV (O) was assigned to O²⁻ in the catalysts lattice, whereas the binding energy at 532.0-532.2 eV (O') was assigned to surface adsorbed oxygen such as O⁻ or OH⁻. The binding energy about 533.5-533.8 eV (O'') was associated with adsorbed molecular water. Usually, a higher oxygen ad-species concentration on the catalyst surface is beneficial to the enhancement in catalytic activity [23, 24]. The relative content of the surface adsorbed oxygen species in the total surface oxygen can be estimated from the relative area of the sub-peak, the results are shown in Table 3. The surface adsorbed oxygen concentration of Pd-Fe/meso-C sample calcined at 60-400 °C was following:

Pd-Fe/meso-C-100 (13.60)> Pd-Fe/meso-C-400 (8.80)> Pd-Fe/meso-C-200 (5.48)> Pd-Fe/meso-C-300 (4.42).

Though above mention research, tetravalent Pd and Fe species of catalyst surface were main active component and oxygen storage material in Pd-Fe/meso-C catalysts, respectively. When existing form of Fe species was identical, the higher the surface tetravalent Pd content is, the higher the activity of catalysts is. So the Pd-Fe/meso-C-200 catalyst had higher activity than the Pd-Fe/meso-C-100 catalysts. When existing form of Fe species was distinct, it had an important influence in activity of CO catalytic oxidation. As we all know, The oxygen storage capacity of FeO(OH) was outclassed Fe₂O₃. When Pd loading content was similar, the higher oxygen storage capacity is, the higher the activity of catalysts is. So the Pd-Fe/meso-C-200 catalyst had highest activity than Pd-Fe/meso-C-400 and Pd-Fe/meso-C-300 catalysts.

3.5 The effect of moisture on the performance of catalyst

Moisture played negative effects on CO conversion, which was because the competitive adsorption of gaseous water that hindered CO activation and benefited to the formation of carbonates under the saturated moisture condition. Moisture is inevitably existed in practical applications especially at low temperature. Thus, it is more important to study the catalytic behavior of the superior Pd-Fe/meso-C catalyst under moisture condition, the result of which was seen in Fig.9. It was found that T₁₀₀ had no obvious changes in the presence or the absence of moisture in feed gas. The superior Pd-Fe/meso-C catalyst could maintain its activity in 720 min. This indicated

that the catalyst expressed the excellent resistance to moisture.

To investigate moisture on CO oxidation, the Pd-Fe/meso-C catalyst before and after moisture reaction were characterization by XPS, the Pd-Fe/meso-C catalyst after hydrothermal reaction was marked as Pd-Fe/meso-C-H catalyst.

Fig.10 shows the XPS spectra of Pd-Fe/meso-C and Pd-Fe/meso-C-H catalysts. Fig.10A shows the Pd element on the surface of Pd-Fe/meso-C and Pd-Fe/meso-C-H catalysts. After hydrothermal reaction, two palladium species (bivalent Pd and tetravalent Pd) were appeared in Fig.10A(b), which indicated that the Pd species was reduction in CO catalytic oxidation reaction. The Pd loading content of catalysts surface had on much change before and after hydrothermal reaction. But the tetravalent Pd loading content on surface of Pd-Fe/meso-C catalyst was reduced after hydrothermal reaction (seen Table 4). This fact once again showed the tetravalent Pd was main active content in Pd-Fe/meso-C catalysts on CO oxidation.

Fig.10B shows the O element on the surface of Pd-Fe/meso-C and Pd-Fe/meso-C-H catalysts. Three peaks (O, O', O'') also were appeared on the surface of Pd-Fe/meso-C and Pd-Fe/meso-C-H catalysts. The O_{ads} content of Pd-Fe/meso-C and Pd-Fe/meso-C-H catalyst surface was similar, but the O_{latt} content of Pd-Fe/meso-C-H catalyst surface was much less than O_{latt} content of Pd-Fe/meso-C catalyst surface after hydrothermal reaction (Table 4), which was illustrated that the lattice oxygen of FeO(OH) species was main reaction route in the reaction of CO oxidation.

The total results showed that surface area, surface adsorbed oxygen

concentration, surface loading content and the existing forms of Pd and Fe were the key factors influencing the catalytic performance of Pd-Fe/meso-C catalysts [13, 17]. The meso-C sample had superior surface area, external surface area and order pore structure, all of this was helpful for loading of active component and promoter. After loading Pd-Fe, the surface area, external surface area was decreased, which indicated that the active component and promoter was loaded in surface and pore channel of meso-C sample. The activity influence factor of Pd-Fe/meso-C catalyst was investigated in detail. The superior prepared condition of catalyst on CO oxidation was chosen: at 0.625 wt.% Pd loading content, pH value was 8.5, calcined temperature was 200 °C, the catalyst possessed highest activity of CO oxidation. The superior Pd-Fe/meso-C catalyst exhibited the excellent resistance to moisture.

Compared with the result of catalyst activity and catalyst characterization, it was discovered that tetravalent Pd was main active component, the Fe species was main oxygen storage materials. Though analyzing, the surface tetravalent Pd content was main influence factor when existing form of Fe species was identical, and the existing form of Fe species was main effect factor when surface tetravalent Pd content was similar. So the reaction mechanism of Pd-Fe/CSs-PVP catalysts on CO oxidation maybe adhered to the Langmuir-Hinshelwood + Redox mechanism (seen Fig.11): CO firstly was adsorbed onto the tetravalent Pd, the adsorbed CO on Pd species were more easily oxidized to CO₂ by catching the lattice oxygen (route 1 and 2) or adsorbed oxygen (route 3), meanwhile the catalysts produced the oxygen vacancy, The oxygen vacancy would be replenished by O₂ of reaction gas to form the new

active oxygen species and complete the redox cycle.

To investigate the economics and practical of Pd-Fe/meso-C catalyst, the activity of similar catalysts was listed in Table 5. T_{100} was 40, 20, 30, and 25, respectively, corresponding to Pd-Cu/Al₂O₃-573 [26], Pd-Fe-Ox/CeO₂-CP-R [8] and Pd-Fe/CSs-PVP-S [27] and Pd-Fe/meso-C catalysts. The CO conversion of Pd-Fe/meso-C catalyst had superior than Pd-Cu/Al₂O₃-573 and Pd-Fe/CSs-PVP-S catalysts under similar conditions. The activity of Pd-Fe-Ox/CeO₂-CP-R catalyst was higher than Pd-Fe/meso-C catalyst because of the higher Pd loading content (1.9 wt.%). In summary, the Pd-Fe/meso-C catalyst possessed lower Pd loading content, high catalytic activity, which was beneficial for future scaled-up route of the Pd-Fe/meso-C catalyst.

4 Conclusions

The meso-C was successfully synthesized by adopting the mesoporous silica KIT-6 as templates. The meso-C exhibited superior surface area, and the external surface area of meso-C sample far higher than microporous area, which meant that the meso-C support was a large number mesoporous and a little microporous. After loading Pd-Fe, the surface area and external surface area of sample had fallen, the microporous area was even disappeared. This indicated that Pd-Fe was loaded on meso-C support surface and pore channel. This study demonstrated that Pd-Fe/meso-C catalysts exhibited CO catalytic performance. It was found that the catalytic performance was significantly influenced by pH value of catalyst, Pd loading content and calcined temperature. At 0.625 wt.%, pH value = 8.5, the Pd-Fe/meso-C

catalyst calcined at 200 °C showed the superior performance. Through analyzing, the surface tetravalent Pd content was main influence factor when existing form of Fe species was identical, and the existing form of Fe species was main effect factor when surface tetravalent Pd content was similar. The reaction pathway of Pd-Fe/meso-C catalysts on CO oxidation maybe adhered to the Langmuir-Hinshelwood + Redox mechanism according to the detailed analysis and characterization.

Acknowledgements

The financial support of The National Basic Research Program of China (2013CB933201), The National Natural Science Foundation of China (21407154, 21507137), The Science and Technology Program of Lanzhou city (2014-2-5) and West Light Foundation of The Chinese Academy of Sciences is gratefully acknowledged.

References

- [1] H. Na, T. Zhu, Z. Liu, *Catal. Sci. Technol.*, 4 (2014) 2051-2057.
- [2] F. Hai, Y. Li, F. Bai, Sagala, Zhaorige, Zhaorigetu, M. Jia, *J. Mol. Catal. (China)*, 21 (2007) 329-332.
- [3] Y. Feng, X. Zheng, *Nano Lett.* 10 (2010) 4762-4766.
- [4] L.D. Socaciu, J. Hagen, T.M. Bernhardt, L. Wöste, U. Heiz, H. Häkkinen, U. Landman, *J. Am. Chem. Soc.*, 125 (2003) 10437-10445.
- [5] J. Hagen, L.D. Socaciu, M. Eljazyfer, U. Heiz, T.M. Bernhardt, L. Wöste, *Phys. Chem. Chem. Phys.*, 4 (2002) 1707-1709.

- [6] N.K. Jena, K.R.S. Chandrakumar, S.K. Ghosh, *J. Phys. Chem. C*, 116 (2012) 17063-17069.
- [7] S. Chen, R. Si, E. Taylor, J. Janzen, J. Chen, *J. Phys. Chem. C*, 116 (2012) 12969-12976.
- [8] Y. Shen, G. Lu, Y. Guo, Y. Wang, Y. Guo, L. Wang, X. Zhen, *Catal. Commun.*, 18 (2012) 26-31.
- [9] Y. Bi, L. Chen, G. Lu, *J. Mol. Catal. A: Chem.*, 266 (2007) 173-179.
- [10] A. Satauma, K. Osaki, M. Yanagihara, J. Ohyama and K. Shimizu, *Appl. Catal. B: Environ.*, 132-133(2013) 511-518.
- [11] P. Kast, M. Friedrich, D. Teschner, F. Girgsdies, T. Lunkenbein, R.N. Alnoncourt, M. Behrens, R. Schlögl, *Appl. Catal. A: Gen.*, 502 (2015) 8-17.
- [12] L. Liu, F. Zhou, L. Wang, X. Qi, F. Shi, Y. Deng, *J. Catal.*, 274 (2010) 1-10.
- [13] W. Han, Z. Tang, P. Zhang, G. Lu, *RSC Adv.*, 4 (2014) 23262-23270.
- [14] F.F. Wang, S. Shao, C.L. Liu, C.L. Xu, R.Z. Yang, W.S. Dong, *Chem. Eng. J.*, 264 (2015) 336-343.
- [15] Y. Jo, J.Y. Cheon, J. Yu, H.Y. Jeong, C.H. Han, Y. Jun, S.H. Joo, *Chem. Commun.*, 48 (2012) 8057-8059.
- [16] K. Ariga, Y. Yamauchi, G. Rydzek, Q. Ji, Y. Yonamine, K.C.W. Wu, J.P. Hill, *Chem. Lett.*, 43 (2014) 36-68.
- [17] W. Han, G. Zhang, G. Lu, Z. Tang, *RSC Adv.*, 5 (2015) 59666-59676.
- [18] Y. Li, J. Wei, W. Luo, C. Wang, W. Li, S. Feng, Q. Yue, M. Wang, A.A. Elzatahry, Y. Deng, D. Zhao, *Chem. Mater.*, 26 (2014) 2438-2444.

- [19] Katsuhiko Ariga, Ajayan Vinu, Yusuke Yamauchi, Qingmin Ji, Jonathan P. Hill, *Bull. Chem. Soc. Jpn.*, 85 (2012) 1-32.
- [20] H. Liu, L.H. Jin, P. He, C. Wang, Y. Xia, *Chem. Commun.*, 44 (2009) 6813-6815.
- [21] Y. Su, Z. Tang, W. Han, P. Zhang, Y. Song, G. Lu, *CrystEngComm*, 16 (2014) 5189-5197.
- [22] K. S. Kim, A. F. Gossmann, N. Winograd., *Anal. Chem.*, 46 (1974) 197-200.
- [23] C.D. wagner, W.M. Riggs, L.E. Davis, J.F. Moulder, G.E. Muilenberg, *Handbook of X-Ray Photoelectron Spectroscopy*, Physical Electronics Inc, USA, 1995.
- [24] Z.M. Liu, J.M. Hao, L.X. Fu, T.L. Zhu, *Appl. Catal. B: Environ.*, 44 (2003) 355-370.
- [25] Z. Qu, F. Yu, X. Zhang, Y. Wang, J. Gao, *Chem. Eng. J.*, 229 (2013) 522-532.
- [26] E.M. Slavinskaya, R.V. Gulyaev, A.V. Zadesenets, O.A. Stonkus, V.I. Zaikovskii, Y.V. Shubin, S.V. Korenev, A.I. Boronin, *Appl. Catal. B: Environ.*, 166-167 (2015) 91-103.
- [27] W. Han, Z. Tang, P. Zhang, G. Lu, *Appl. Surf. Sci.*, 350 (2015) 100-108.

Figure and Table Captions:

Table 1 Pore structure parameters of meso-C and Pd-Fe/meso-C sample

Sample	BET Surface area (m^2g^{-1})	Micropore Area (m^2g^{-1})	External surface area (m^2g^{-1})	Pore volume (cm^3g^{-1})	Average pore diameter (nm)
Meso-C	699.50	62.04	637.46	0.61	3.46
Pd-Fe/meso-C	509.24	-	497.93	0.46	3.61

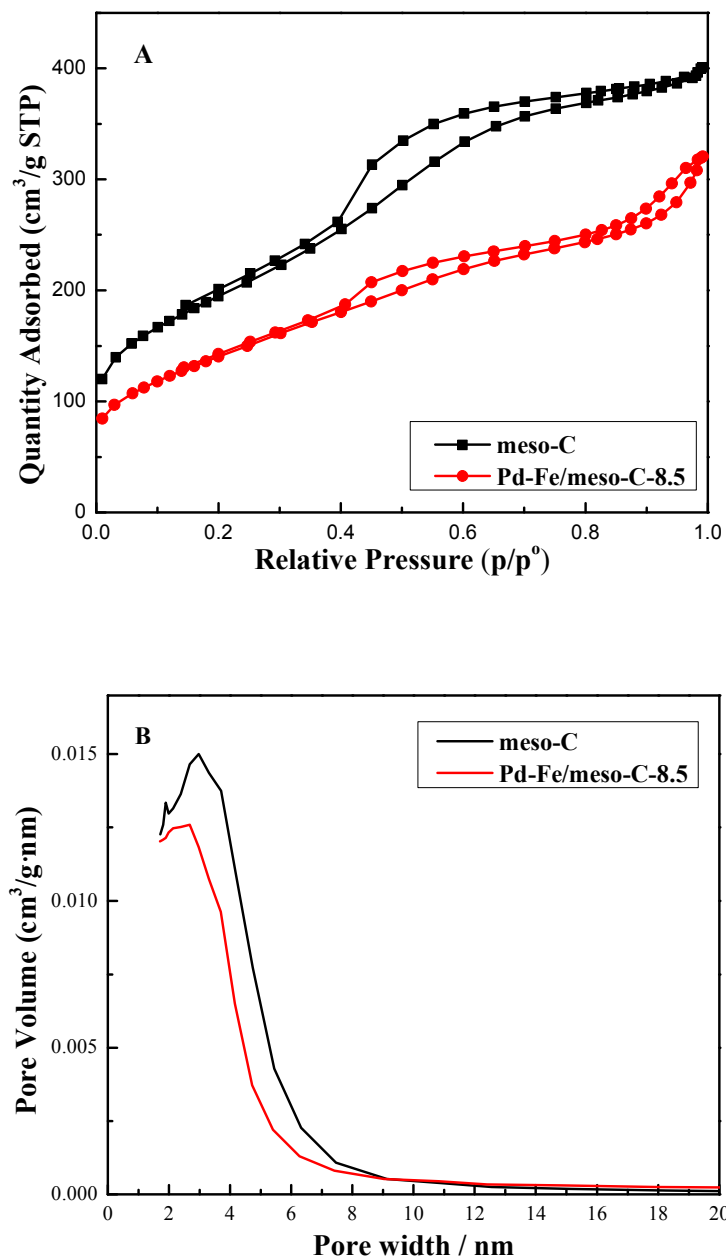


Fig.1 N₂ adsorption-desorption isotherms (A) and BJH pore size distributions (B) of meso-C and Pd-Fe/meso-C-8.5.

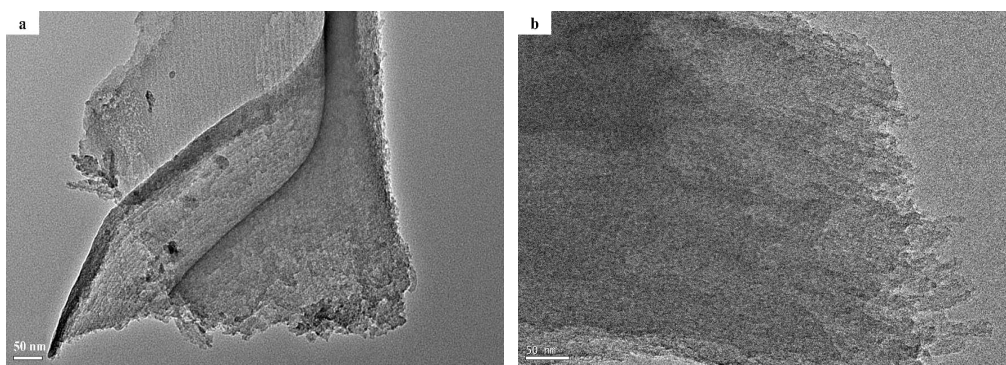


Fig.2 TEM images of meso-C (a) and Pd-Fe/meso-C (b).

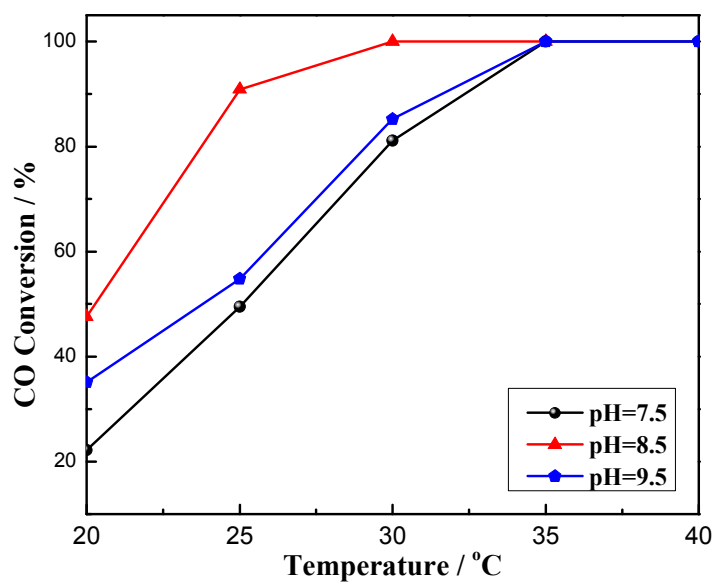


Fig.3 Catalytic activity of Pd-Fe/meso-C catalysts prepared by various pH values.

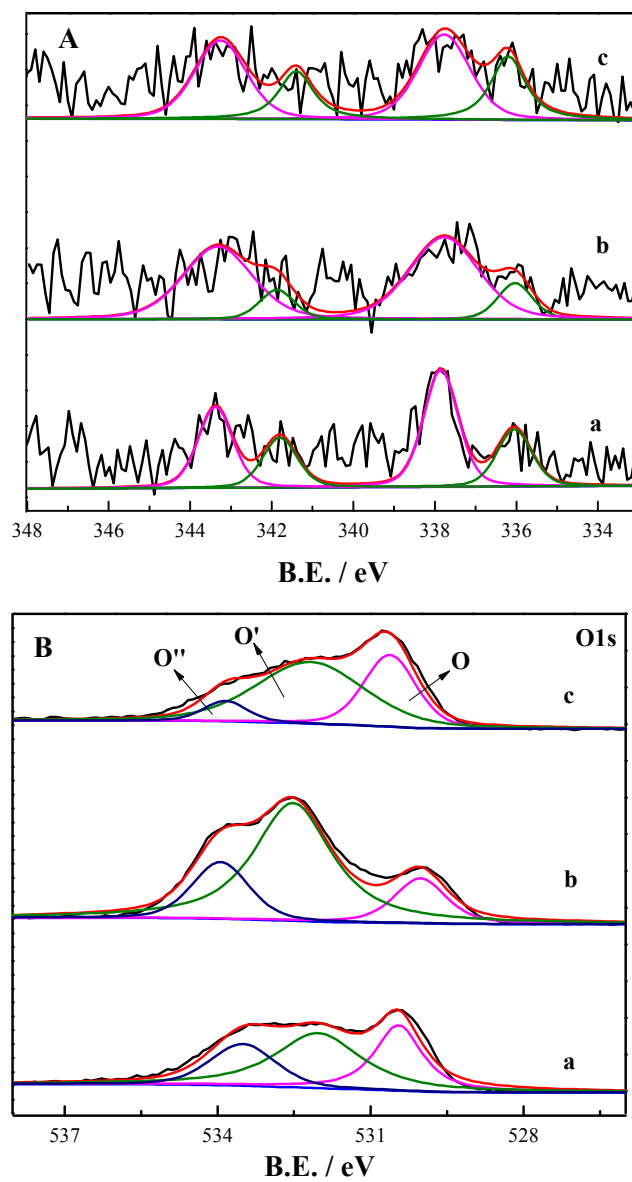


Fig.4 (A) Pd3d and (B) O 1s XPS spectra of Pd-Fe/meso-C catalysts prepared by various pH values: (a) pH=7.5; (a) pH=8.5; (a) pH=9.5.

Table 2 Chemical properties of Pd-Fe/meso-C catalysts prepared by various pH values

Sample	pH value	$O_{\text{ads}}/(O_{\text{ads}} + O_{\text{latt}})$ or $(O' + O'')/(O + O' + O'')$	Pd^{4+} $/(Pd^{4+} + Pd^{2+})$	O content (%)	Pd content (%)
Pd-Fe/meso-C	7.5	0.470	0.551	6.48	0.135
Pd-Fe/meso-C	8.5	0.659	0.825	16.48	0.200
Pd-Fe/meso-C	9.5	0.590	0.645	9.20	0.160

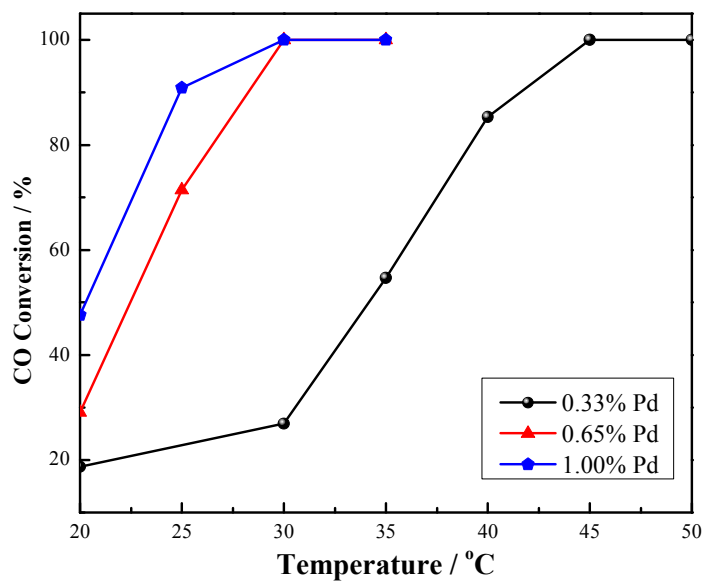


Fig.5 Catalytic activity of Pd-Fe/meso-C catalysts prepared by different Pd loading content.

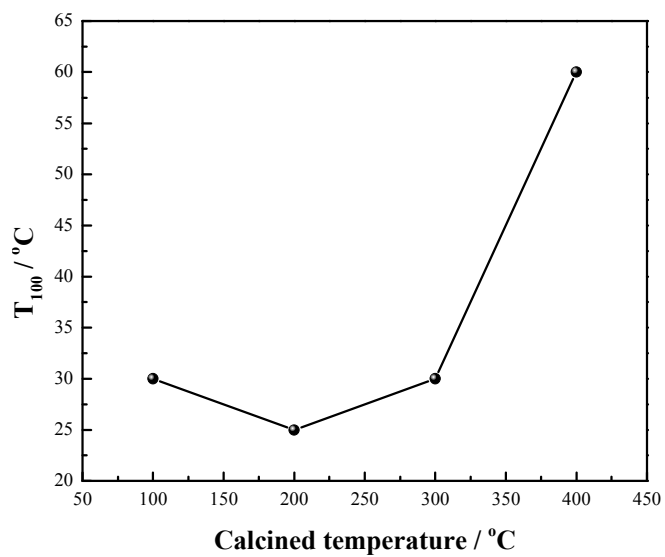


Fig.6 Catalytic activity of Pd-Fe/meso-C catalysts prepared by different calcined temperature.

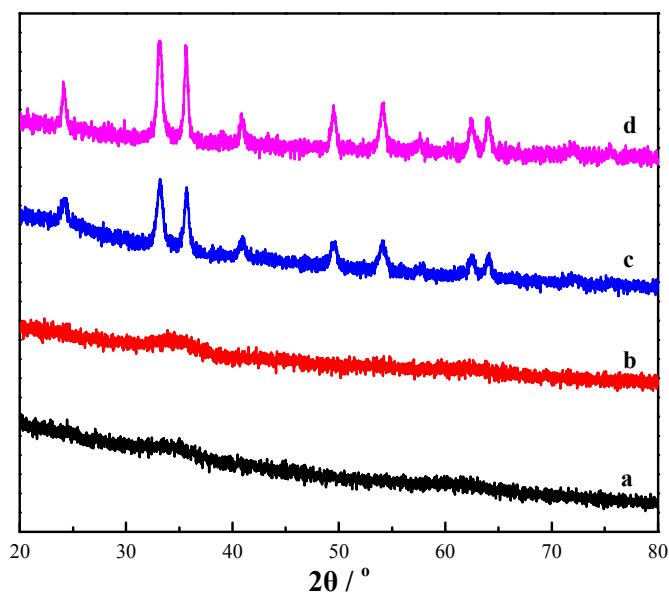


Fig.7 Wide-angle XRD patterns of Pd-Fe/meso-C catalysts prepared by different calcined temperature: (a) 100 °C; (b) 200 °C; (c) 300 °C; (d) 400 °C.

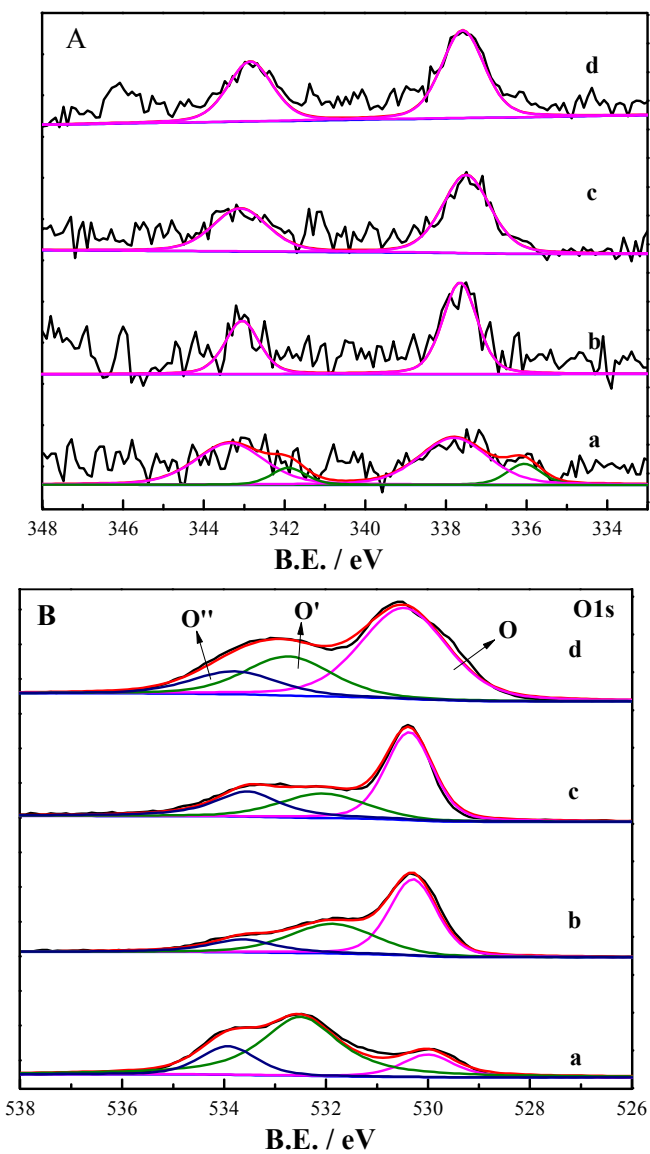


Fig.8 (A) Pd3d and (B) O 1s XPS spectra of Pd-Fe/meso-C catalysts prepared by different calcined temperatures: (a) 100 °C; (b) 200 °C; (c) 300 °C; (d) 400 °C.

Table 3 Chemical properties of Pd-Fe/meso-C catalysts prepared by different calcined temperature

Sample	Calcined temperature (°C)	$O_{\text{ads}}/(O_{\text{ads}} + O_{\text{latt}})$ or $(O' + O'')/(O + O' + O'')$	$Pd^{4+}/(Pd^{4+} + Pd^{2+})$	O content (%)	Pd content (%)
Pd-Fe/meso-C	100	0.825	0.825	16.48	0.200
Pd-Fe/meso-C	200	0.354	1.000	15.49	0.246
Pd-Fe/meso-C	300	0.256	1.000	17.27	0.250
Pd-Fe/meso-C	400	0.256	1.000	34.39	0.273

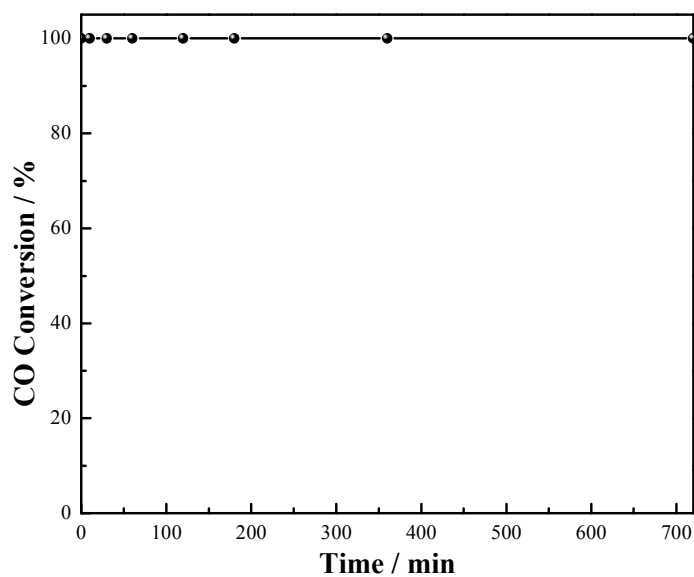


Fig.9 The effect of moisture on CO oxidation. Reaction conditions: under moisture and 1% CO balance air, WHSV = 10,000 mlh⁻¹g⁻¹.

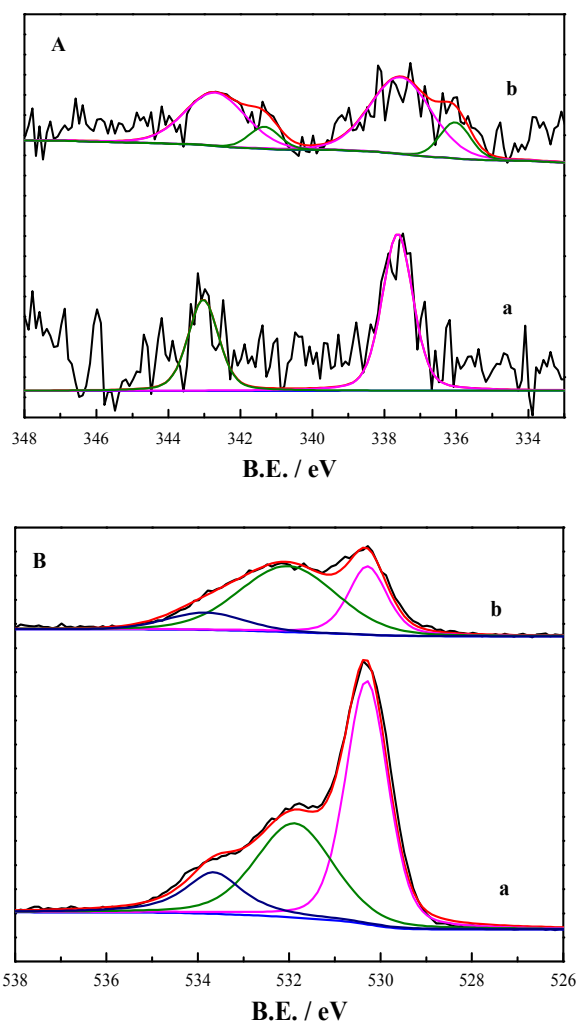


Fig.10 (A) Pd3d and (B) O 1s XPS spectra of Pd-Fe/meso-C and Pd-Fe/meso-C-H catalysts.

Table 4 Chemical properties of Pd-Fe/meso-C and Pd-Fe/meso-C-H catalysts

Sample	$O_{\text{ads}}/(O_{\text{ads}} + O_{\text{latt}})$ or $(O^{\cdot} + O^{\cdot\cdot})/(O + O^{\cdot} + O^{\cdot\cdot})$	Pd^{4+} $/(Pd^{4+} + Pd^{2+})$	O content (%)	Pd content (%)
Pd-Fe/meso-C	0.354	1.000	15.49	0.246
Pd-Fe/meso-C-H	0.724	0.817	9.22	0.240

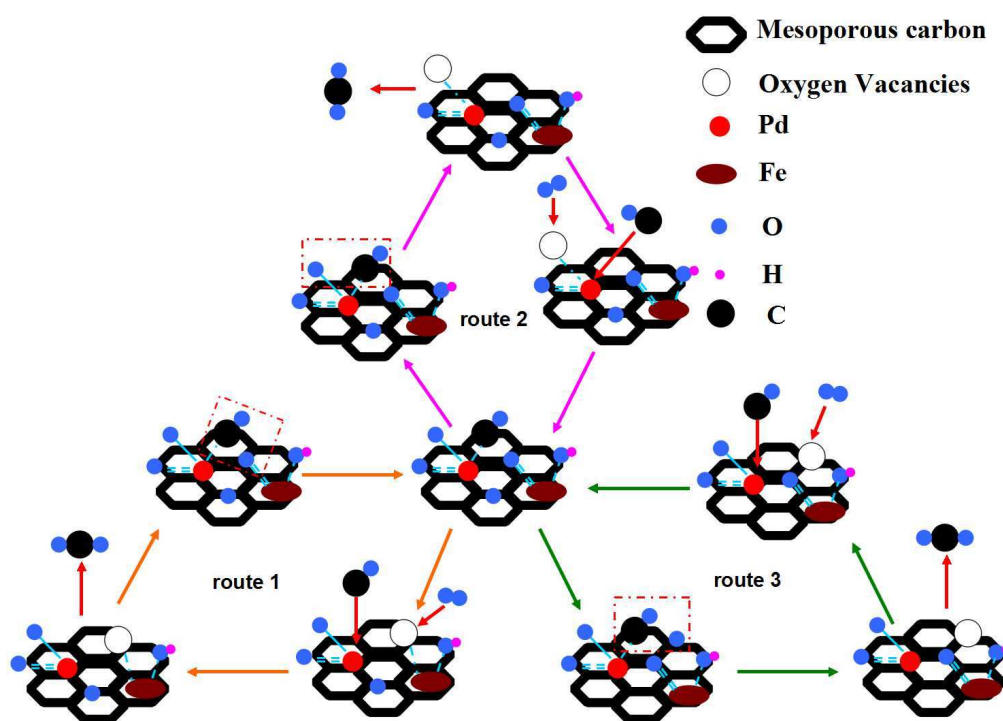


Fig.11 Reaction pathway illustration for CO oxidation over Pd-Fe/meso-C catalysts.

Table 5 Compare of different Pd supported catalysts on activity of CO oxidation.

Catalysts	Method	Pd Loading (%)	Reaction condition	T ₁₀₀ (°C)	Ref
Pd-Cu/Al ₂ O ₃ -573	IM	1.90	0.5-1.0g catalyst, feed gas 50-100ppm CO	40	[26]
Pd-Fe-Ox/CeO ₂ -CP-R	DP	1.90	0.2g catalyst, feed gas 1 vol.% CO	20	[8]
Pd-Fe/CSs-PVP	DP	1.25	0.3g catalyst, feed gas 1 vol.% CO	30	[27]
Pd-Fe/meso-C	DP	0.625	0.3g catalyst, feed gas 1 vol.% CO	25	This work

IM: Impregnation method; DP: Deposition precipitation method.